





Research Article

Study on Zonal Cooperative Control Technology of Surrounding Rock of Super Large Section Soft Rock Chamber Group Connected by Deep Vertical Shaft

Shengrong Xie ¹, Zaisheng Jiang ¹, Dongdong Chen ¹, and En Wang ^{1,2}

¹School of Energy and Mining Engineering, China University of Mining and Technology, Beijing 100083, China

²Department of Civil Engineering, The University of British Columbia, Vancouver, British Columbia V6T1Z4, Canada

Correspondence should be addressed to Dongdong Chen; chendongbcg@163.com

Received 26 February 2022; Accepted 16 May 2022; Published 14 June 2022

Academic Editor: Junwei Ma

Copyright © 2022 Shengrong Xie et al. This is an open access article distributed under the Creative Commons Attribution License, which permits unrestricted use, distribution, and reproduction in any medium, provided the original work is properly cited.

Aiming at solving the problem of asymmetric deformation, failure, and stability control of surrounding rock caused by the excavation of deep super large section soft rock chamber group passing through multilayer strata, taking super large section soft rock chamber group connected by deep vertical shaft in Wuyang Coal Mine as the engineering background, the deformation development mode of surrounding rock, the expansion situation of loosening range, and the plastic failure response characteristics in chamber group under the disturbance influence are monitored and numerically analyzed. On this basis, the super large section chamber group is divided into four maintenance control areas: area I (severe deformation area), area II (stable deformation area), area III (medium deformation area), and area IV (small deformation area), and the asymmetric deformation and failure mechanism of the surrounding rock of the chamber group is analyzed. The influence mechanism of specific support technologies on the deformation control effect of surrounding rock of chamber group is systematically studied, including high-strength prestressed bolt (cable) mesh shotcreting coupling support technology, reinforced concrete wall subarea brickwork support technology, and hollow bolt (cable) grouting reinforcement technology of fragmented coal and rock mass. The basic control ideas and technical methods of surrounding rock of deep large section soft rock chamber group are formed. The subarea collaborative control technology of “high-strength prestressed bolt (cable) mesh shotcreting coupling + reinforced concrete wall brickwork support technology + high-strength bolt (cable) grouting of fragmented coal and rock mass” is proposed. The field application shows that this technology realizes effective control of surrounding rock of super large section chamber group.

1. Introduction

With the development of coal mine towards deep large-scale, there are more and more large section soft rock chamber group [1–5]. The excavation of large section soft rock chamber group is an irreversible dynamic evolution process of nonlinear and large deformation mechanics [6–10]. Especially in the deep complex conditions, chamber group excavation can lead to the formation of a large range of surrounding rock fracture area in a short time, so that the bearing capacity of surrounding rock itself is reduced, which is prone to full section roof fall, coal side spalling, and other dynamic damage accidents, seriously affecting the safety construction of the mine [11–14].

For this reason, many scholars have done a lot of studies on the failure mechanism and control technology of large section chamber group. Zhang et al. evaluated the chamber group stability using the risk analysis method, and the risk management stages were divided into two main stages: initial risk management and dynamic and final risk management [15]. Ding et al. established a transversely-isotropic elastoplastic constitutive model for large underground chamber group excavated in layered rock masses with steep dip angles, and the numerical simulations were performed during the construction process [16]. Wang et al. analyzed the stability of the chamber group using the element safety factor method, and the permeabilities of the anhydrite intact rock and rock mass were estimated based

on laboratory and field tests [17]. Zhang et al. developed a user-defined constitutive model with the Hoek-Brown failure criterion, and the model for the anhydrite chamber group is established to analyze the stability used for underground oil storage [18]. Huang et al. carried out the numerical experiment of different cross section size, chamber spacing, and construction sequence; the construction disturbance mechanism was clarified; and the optimal excavation sequence of coal bunker chamber group was obtained [19]. Wang et al. established the evaluation indexes of surrounding rock control rate and deformation coordination rate, and the optimization design method of deep large section chamber is put forward [20]. Xu et al. proposed a method of intelligent autofeedback and safety early-warning for underground chamber group based on BP neural network and FEM [21]. Qian and Zhou proposed the general rules and reinforcement method for zonal disintegration of the surrounding rock masses during excavation of underground chamber group under high in situ stresses [22]. Liu et al. studied the deformation and evolution laws of the surrounding rock of a triangle-shaped chamber group under different dynamic loads using a similar simulation test [23]. Zhou et al. established the quantitative evaluation indexes of surrounding rock control rate and deformation coordination rate, and the numerical test research is carried out under the influence factor [24]. Tan et al. researched the stress, deformation, and failure characteristics of the in-site chamber group surrounding rock, and the optimum chamber group parameters are determined [25]. Zhang et al. divided the excavation process of the chamber group into three phases, and the construction optimization scheme is formulated. The stress and plastic zone of each excavation scheme are analyzed [26].

The achievements of many experts and scholars have promoted the development of study on failure and control technology of deep large section chamber groups. The deformation and failure of deep large section chamber groups usually presents asymmetric characteristics. Its stability cannot be guaranteed by using conventional full section equal strength symmetrical support forms. Therefore, on the basis of previous studies, taking super large section soft rock chamber group connected by deep vertical shaft in Wuyang Coal Mine as the engineering background, this paper divides the maintenance control area of the deep super large section chamber group and analyzes the asymmetric deformation and failure mechanism of the surrounding rock of the chamber group. The influence mechanism of specific support technologies on the deformation control effect of surrounding rock of chamber group is systematically studied, which include high-strength prestressed bolt (cable) mesh shotcreting coupling support technology, reinforced concrete wall subarea brickwork support technology, and hollow bolt (cable) grouting reinforcement technology of fragmented coal and rock mass. The basic control ideas and technical methods of surrounding rock of deep large section soft rock chamber group are determined, and the corresponding subregional collaborative control technology is formed.

2. Project Overview

Nanfeng working area of Wuyang Coal Mine is located in Changzhi City, Shanxi Province, China. The development mode is shaft development, as shown in Figure 1. The normal water inflow of the mine is $305 \text{ m}^3/\text{h}$, and the maximum water inflow of the mine is $469 \text{ m}^3/\text{h}$. It is classified as a mine with medium hydrogeological conditions. A total of 5 normal faults are found in Nanfeng working area of Wuyang Coal Mine. The fault is far away from the chamber group and does not constitute an impact. In order to meet the application demand of large equipment in coal mine, many large section chambers and roadways are designed and constructed at the site connected with deep shaft, forming many large section chamber groups.

The large section chamber group connected with deep shaft is located under the 3# coal seam, with a buried depth of about 760 m. The main chambers include shaft, horse-head, 1# hydraulic station chamber, 2# hydraulic station chamber, control chamber, and waiting chamber. The geological conditions of the chamber group are complex. During the construction process, the strata that the chamber group passes through are sandy mudstone, fine-grained sandstone, thin mudstone, and sandy mudstone. The chamber group passes through multilayer rocks, and the surrounding rock of the chamber group, especially the roadway roof rock mass, presents obvious soft rock characteristics: broken and loose, poor integrity, and low strength. According to standard for engineering classification of rock mass (GB/T50218-2014), the surrounding rock of chamber group is classified as V-Class unstable rock. The cross section area of each chamber is generally large, and the maximum cross section area of section 5-5 is more than 88 m^2 , which is a typical super large section chamber in deep soft rock. The lithology and typical large section chamber parameters of the chamber group are shown in Figure 2.

3. Deformation and Failure Characteristics and Mechanism Analysis of Deep Large Section Soft Rock Chamber Group

3.1. Analysis of Deformation and Failure Characteristics of Chamber Group

3.1.1. Analysis of In Situ Deformation Characteristics of Surrounding Rock. In order to master the deformation situation of the chamber group, the measuring line is set to monitor the convergence state of surrounding rock. Figure 3(a) shows the relative convergence change of roof-to-floor at different positions along the roadway axis after 26 days of initial support, and Figure 3(b) shows the relative convergence change of roof-to-floor of each chamber with time within 26 days.

It can be seen from Figures 3(a) and 3(b) that the deformation of surrounding rock of large section chamber group connected by deep shaft presents obvious asymmetry. (1) Along the axial direction of the roadway, the convergence of the roof-to-floor increases steadily at first and then increases rapidly. There is no significant difference in the

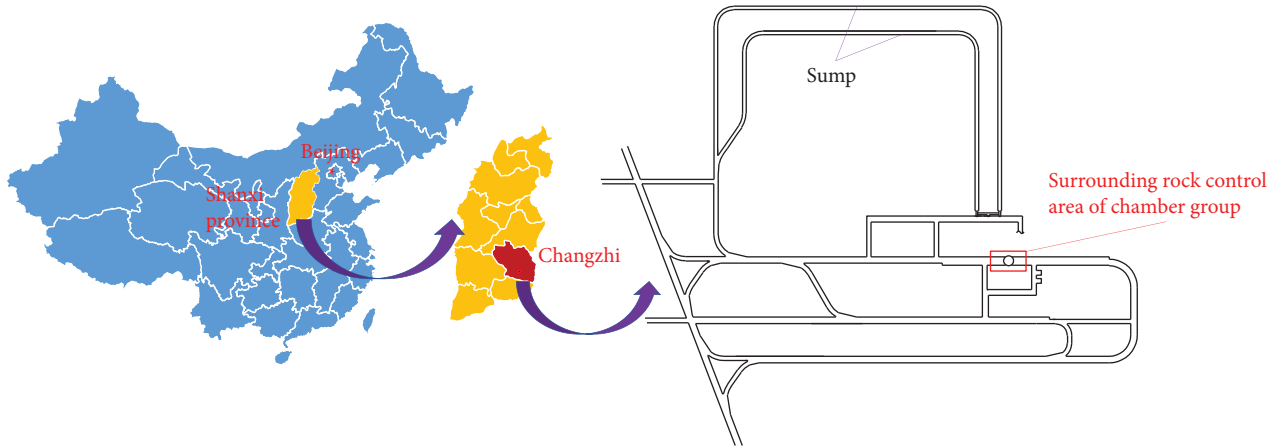


FIGURE 1: Schematic diagram of mine location.

deformation of each section in area II. In area I, the closer to the wellbore, the greater the deformation of surrounding rock. (2) Within 26 days, with the change of time, the deformation of surrounding rock of 1# hydraulic station chamber and waiting chamber (Area IV) is not much different, the deformation of 2# hydraulic station chamber and control chamber (Area III) is not much different, but the deformation of 1# hydraulic station chamber and waiting chamber is smaller than that of 2# hydraulic station chamber and control chamber. (3) According to the deformation trend analysis of the surrounding rock of the each chamber in Figure 3(b), the deformation of the surrounding rock of the chamber is not stable, and there will be continuous large deformation in the future. (4) On the whole, the deformation of the chamber group presents the change rule: area I > area II > area III > area IV.

3.1.2. Analysis on Boreholes Peeping Results. In order to further explore the internal failure of surrounding rock and determine the key support area on the same section in each area, the borehole peeper is used to detect the loose failure range of surrounding rock on typical Section 3-3, and the surrounding rock fracture is shown in Figure 4.

Based on the analysis of borehole peeping detection results, the cracks are densely developed within the depth of 4 m. The surrounding rock of the two sides and the floor above 8 m deep are basically complete, the rock mass is dense, and no obvious cracks are found, while the roof and two shoulders of the roadway within this range are still fractured to a certain depth. It can be seen that the broken degree of roof and two shoulders of surrounding rock is greater than that of two sides. So the roof and two shoulders of surrounding rock is the key supporting part.

3.1.3. Numerical Simulation of Excavation Disturbance of Large Section Chamber Group Connected Deep Shaft. According to the field geological data, the numerical calculation model ($x \times y \times z = 60 \times 63 \times 57$ m) is established, as shown in Figure 5. The overburden self-weight stress of 19 MPa was applied on the model upper part, and the lateral

pressure coefficient is 1.2. The strain softening model is adopted for coal seam, and the Mohr Coulomb model is adopted for other strata. The parameters of coal and rock mass are calculated and analyzed on the basis of indoor measured results.

In order to explore the response evolution law of surrounding rock stress and plastic failure when different areas are excavated in the super large section soft rock chamber group connected by deep vertical shaft, the model adopts the excavation sequence consistent with the actual situation of the field project, that is, the shaft, the variable section super large section roadway (area I) from the waiting chamber (1# hydraulic chamber) to the shaft, the roadway (area II) close to the waiting chamber (1# hydraulic chamber) and gradually away from the shaft, the waiting chamber, 1# hydraulic chamber, and 2# hydraulic chamber and control chamber. The plastic failure response characteristics of surrounding rock after excavation are simulated as shown in Figure 6.

The maximum damage depth of roof, two shoulders, two sides, and floor in area II is kept at 5.3, 5.5, 4.1, and 4.5 m. The maximum damage depth of roof, two shoulders, two sides, and floor of 3-3 profile in area I is kept at 8.0, 8.3, 7.2, and 6.3 m. The maximum damage depth of roadway side of 5-5 profile in area I is kept at 9.2 m. Affected by shaft excavation, the plastic damage range of roof and floor of 5-5 profile in area I is greatly wide.

The damage degree of area I is much higher than that of area II, and the contour line of plastic zone expands to the surrounding rock when it transits from area II to area I. It can be seen that area I is affected by its own large section, excavation disturbance of chamber and shaft, and occurrence of rock stratum, where plastic damage scope is the largest, which is the weakest area of the whole large section chamber group connecting deep shaft, and is the key core area in support design.

According to the plastic zone of typical section in area I and II, the depth of plastic zone of surrounding rock roof and two shoulders is greater than that of the two sides and floor. So roof and two shoulders of roadway are the key support part in surrounding rock control area in areas I and II. The rock column between control chamber and 1#

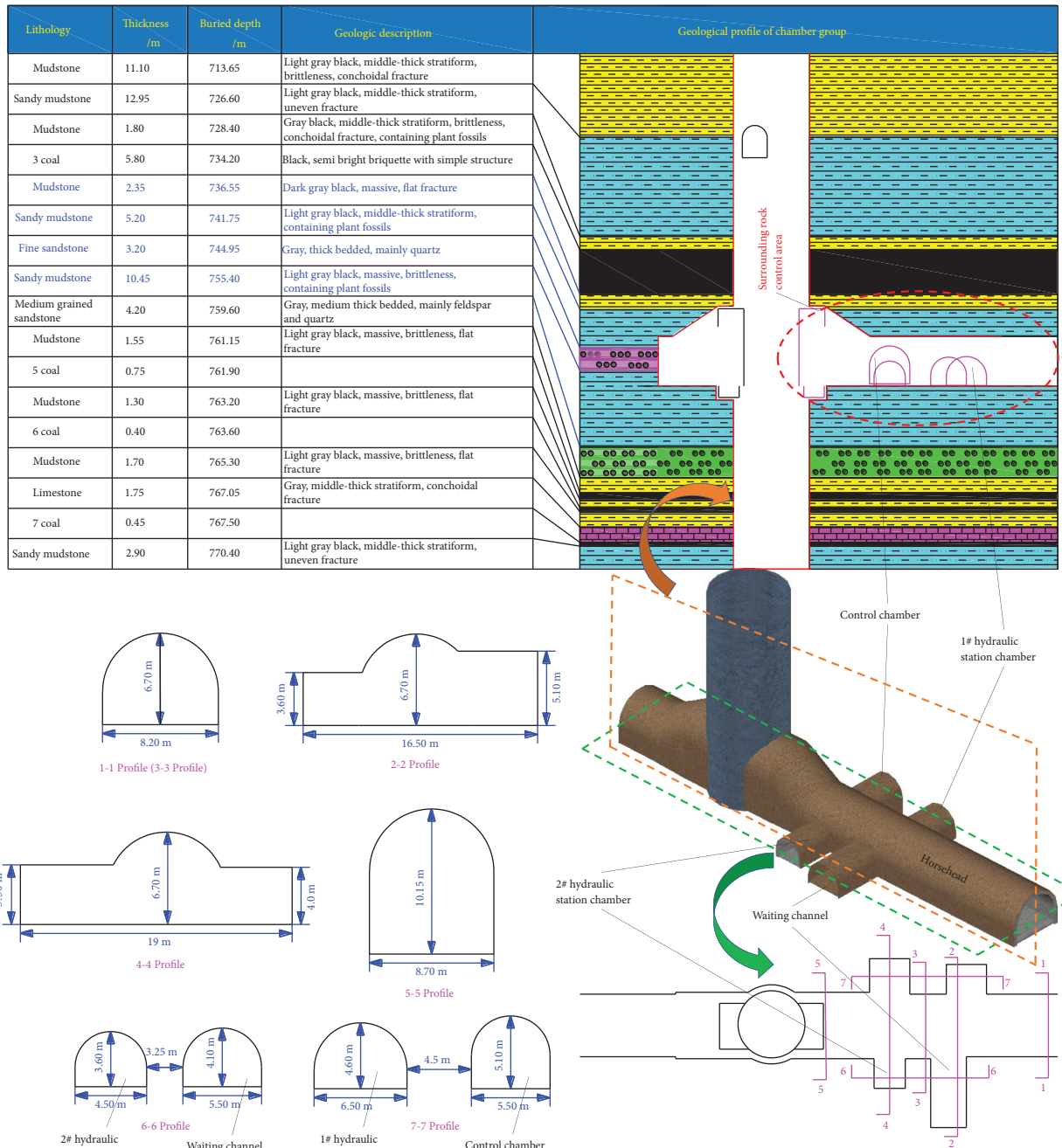


FIGURE 2: Lithology and parameters of typical large section of chamber group.

hydraulic station chamber and between 2# hydraulic station chamber and waiting chamber completely enters into plasticizing state. The contour line of plastic zone shrinks when it transits from area III (including control chamber and 2# hydraulic station chamber) to area IV (including 1# hydraulic station chamber and waiting chamber). The damage scope of control chamber and 2# hydraulic station chamber is larger than that of 1# hydraulic station chamber and waiting chamber, which is the key support chamber area.

To sum up, the deformation, fracture derivation, and plastic failure of surrounding rock in different areas of large

section chamber group connecting deep shaft are different significantly, and the failure degree of rock mass is different in different parts of the same area. Therefore, based on the above analysis, the variable section super large section roadway from the waiting chamber (1# hydraulic chamber) to the shaft can be divided into area I (severe deformation area), the roadway close to the waiting chamber (1# hydraulic chamber) and gradually away from the shaft can be divided into area II (stable deformation area), and the 2# hydraulic chamber and control chamber can be divided into area III (medium deformation area) and 1# hydraulic chamber and waiting chamber are divided into area IV (small deformation

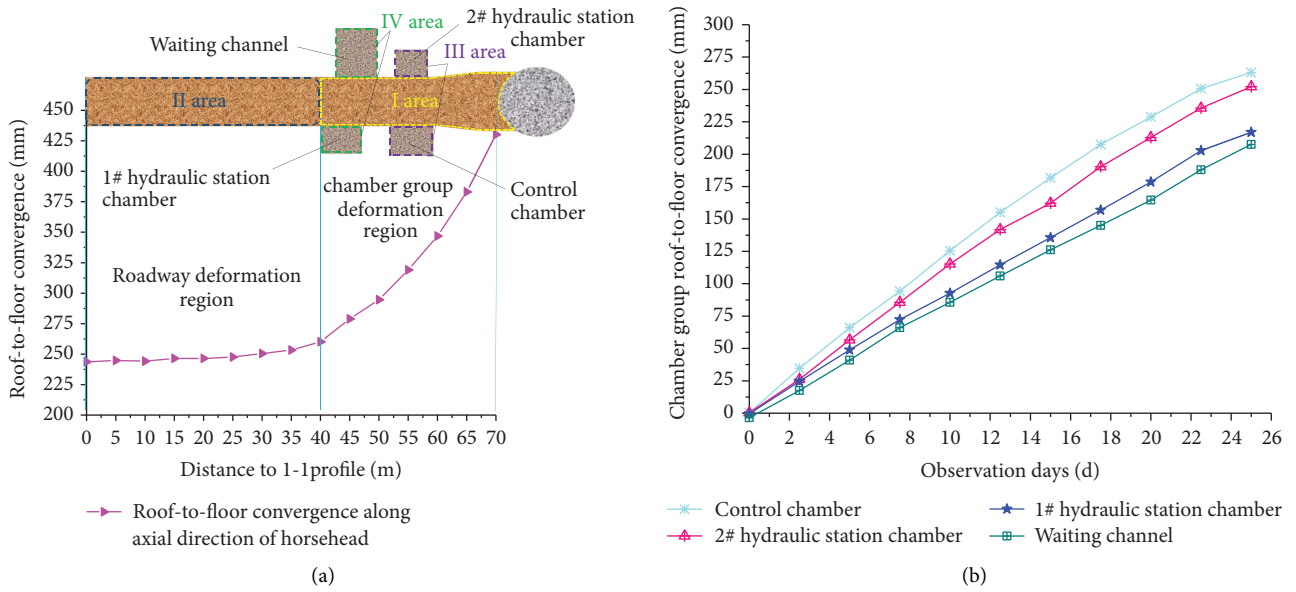


FIGURE 3: Convergence state of surrounding rock: (a) variation of relative convergence of roof-to-floor at different positions along roadway axis. (b) Variation of relative convergence of roof-to-floor of each chamber with time changing.

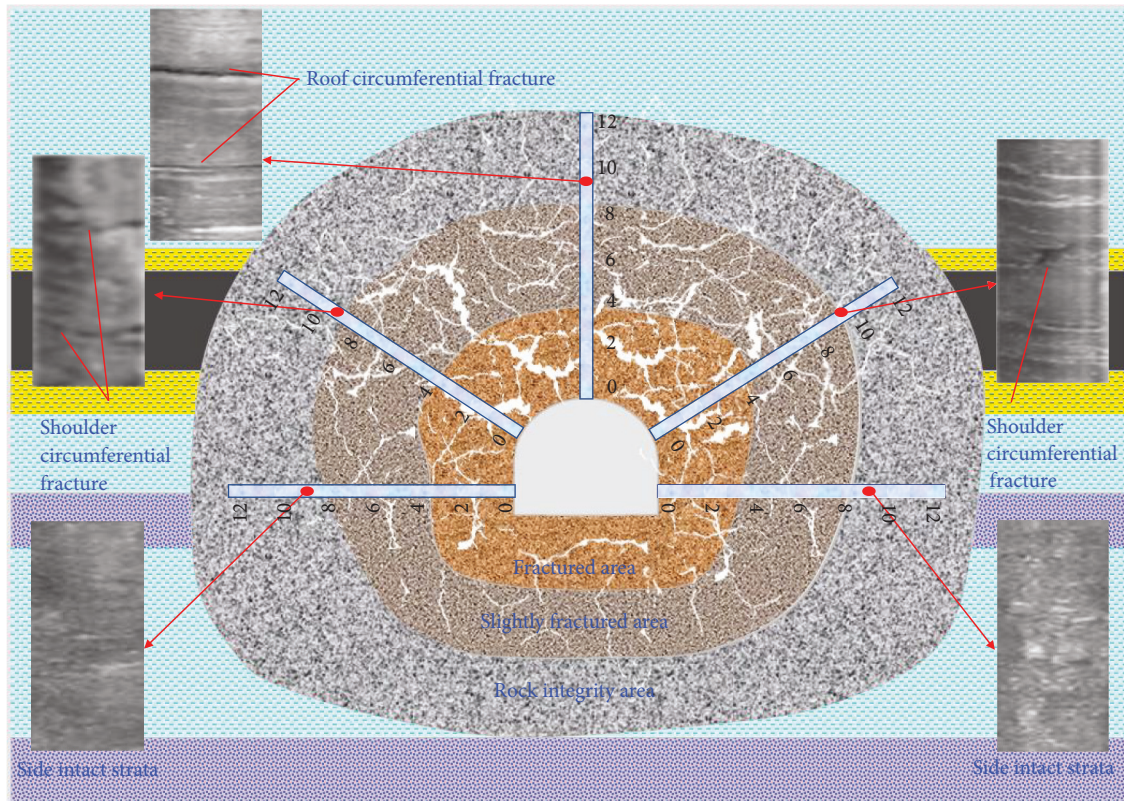


FIGURE 4: Borehole peep and zoning map (unit: m).

area). It can be seen that the broken degree of roof and two shoulders of surrounding rock is greater than that of two sides. So the roof and two shoulders of surrounding rock is the key supporting part (see Figure 7).

3.2. Analysis of Asymmetric Deformation and Failure Mechanism of Chamber Group. The fundamental reasons for the unsymmetrical large deformation of the chamber group are as follows: (1) the cross section of each area of the chamber

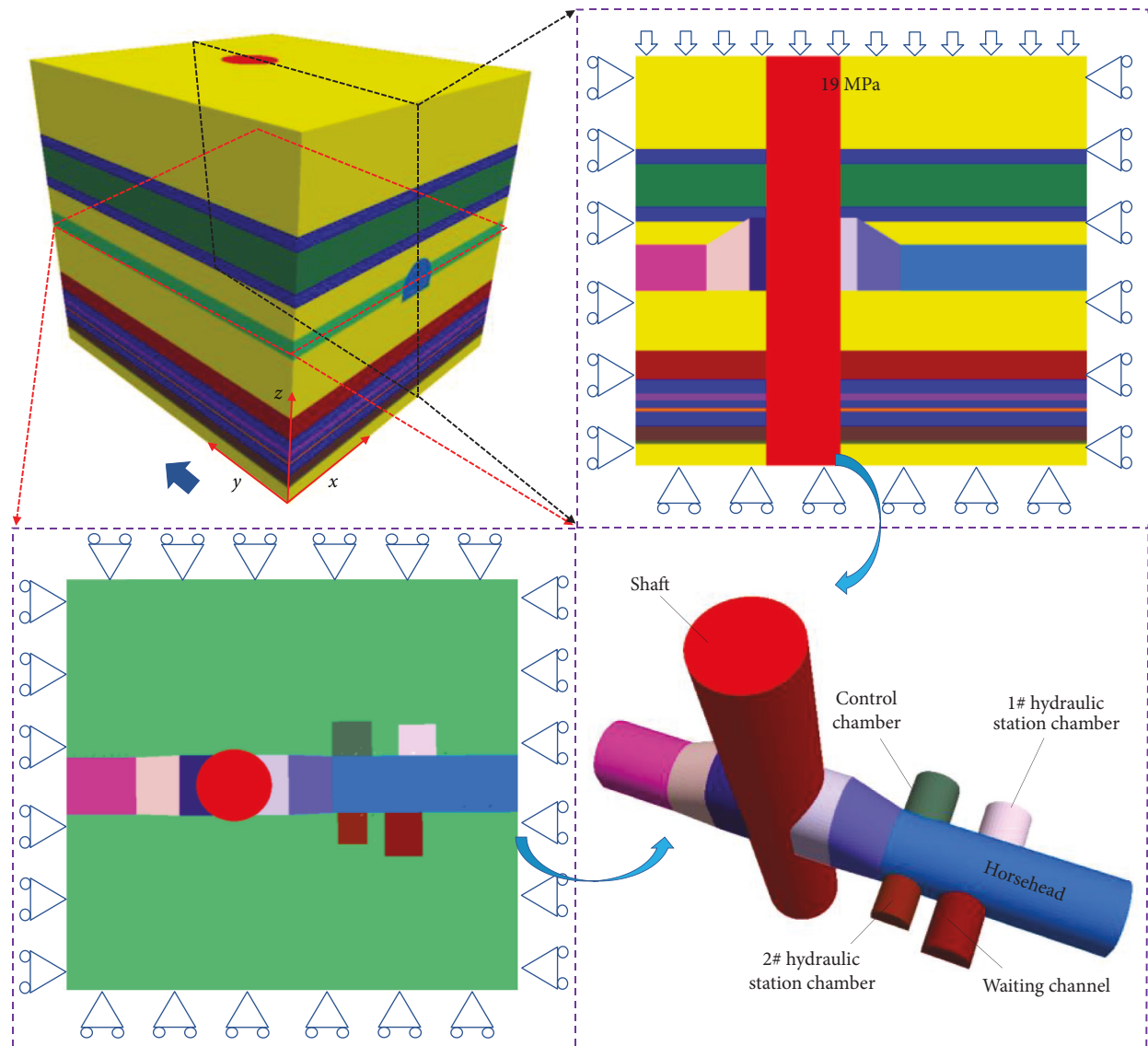


FIGURE 5: Numerical calculation model.

group is large and the size is different, and the surrounding rock is in the complex environment of the chamber group with many free surfaces, vertical and horizontal intersection, and chamber dense layout. (2) Above the two shoulders and roof of the roadway are mudstone thin layer and 3# coal layer, with weak cohesive force, low strength, and stiffness, which is the weak part of surrounding rock. (3) In area I, the large section roadway with variable cross section passes through multilayer rock; the physical and mechanical properties of each rock layer are quite different; the same rock layer also has obvious heterogeneity; and the structural planes such as joints, fissures, and bedding in the surrounding rock are also asymmetric, resulting in obvious asymmetry of lithology and strength distribution. (4) In the deep complex environment, the high deviatoric stress caused by the excavation of chamber group makes the deformation of each area show obvious asymmetric distribution. At the

same time, the important reasons for the obvious regional characteristics of surrounding rock deformation are as follows: (1) the dynamic load disturbance of chamber group is prominent, the structure stress is complex, and the surrounding rock deformation of the chamber group has strong timeliness; (2) roadway is in the state of nonconstant velocity creep for a long time; however, the conventional full section equal strength symmetrical support is used in the original support, which fails to effectively support each part of the roadway. As a result, the support system is gradually damaged by the breakthrough of the support weakness of the chamber group, which makes the surrounding rock locally asymmetric or even full section instability, and then leads to the overall failure trend of the whole deep large section chamber group. The asymmetric deformation and failure mechanism of surrounding rock of chamber group is shown in Figure 8.

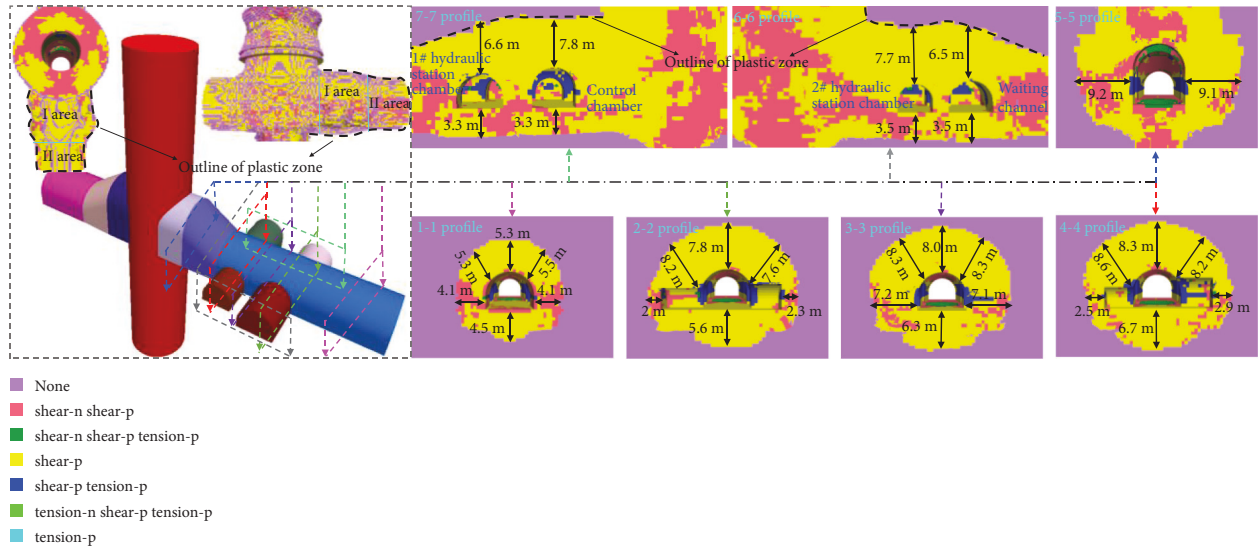


FIGURE 6: Plastic failure response characteristics of surrounding rock after excavation of each chamber.

The damage degree of surrounding rock is from small to large

	IV area	III area	II area	I area
Deformation characteristics (convergence after 26 days)	Small deformation (210 mm)	Medium deformation (253 mm)	Stable deformation (266 mm)	Severe deformation (430 mm)
Fracture concentrated position in each area			Shoulders, roof	Shoulders (>8.0 m), roof (>8.0 m),
Plastic failure concentrated position in each area	Shoulders, roof, rock pillar (plasticization)	Shoulders, roof, rock pillar (plasticization)	Shoulders (5.5 m), roof (5.3 m)	Shoulders (8.3 m), roof (8.0 m)
Classification of each area support grade	Important support area	Important support area	Important support area	Core support area
Key support parts in each area	Shoulders, roof, rock pillar	Shoulders, roof, rock pillar	Shoulders, roof	Shoulders, roof

The area support grade is from small to large

FIGURE 7: Division of maintenance control area and determination of key support position.

4. Surrounding Rock Control Countermeasures and Subarea Cooperative Control Technology

4.1. Control Measures of Surrounding Rock Stability.

Based on this, large cross section chamber group can be divided into I, II, III, and IV four control areas, and the damage degree in each control area is different. Therefore, the surrounding rock control principle should be fully considered deformation and failure characteristics of surrounding rock in different areas. Scientific and reasonable control countermeasures should be taken for different areas, and a new nonequal strength and asymmetric support scheme is formulated to ensure the stability of deep large section chamber group.

4.2. Surrounding Rock Subarea Cooperative Control Technology of Large Section Chamber Group Connected by Deep Shaft

4.2.1. High-Strength Prestressed Bolt (Cable) Mesh Shotcreting Coupling Support Technology. The coupling of high-strength prestressed bolt (cable) (see Figure 9(a)) and surrounding rock will form a high-strength anchorage bearing structure, which is an integral and unified bearing structure formed by bolt support, cable support, and roadway surrounding rock [27, 28], as shown in Figure 9 (b). In the shallow surrounding rock of the roadway, the high-strength anchorage bearing structure is characterized by the mutual extrusion between the bolt and the bolt, forming the principal compression stress circle (as shown

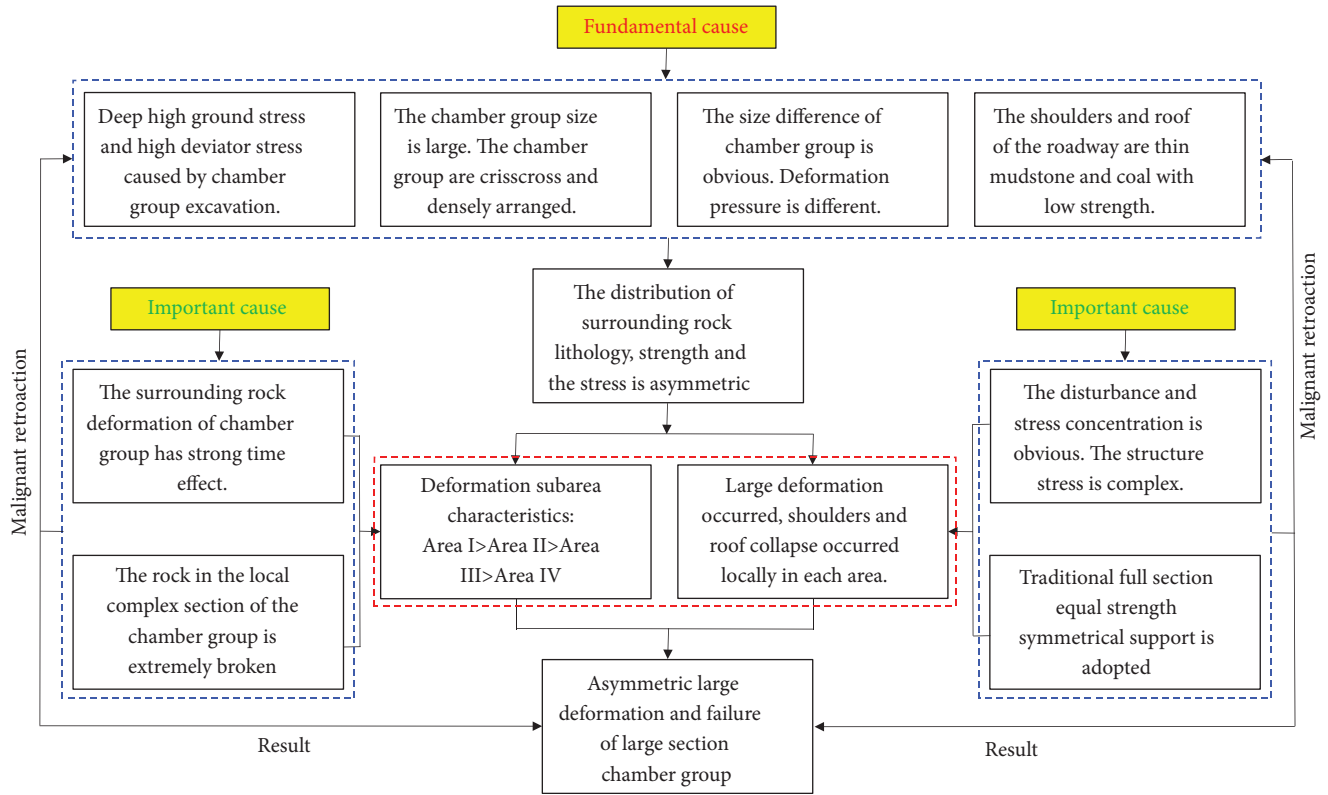


FIGURE 8: Asymmetric deformation and failure mechanism of surrounding rock of chamber group.

in Figure 9 (c)), which has a protective and supporting effect on the rock mass in the shallow surrounding rock fracture area, so that the shallow broken rock mass is not extruded, and then the shallow bolt anchorage bearing structure is formed (as shown in Figure 9 (d)). The application of high-strength prestressed long cable can not only strengthen the shallow bolt bearing structure and exert lateral force on the shallow bearing structure to improve its bearing capacity, but also transfer part of the stress on the bearing body to the deep part of the surrounding rock, forming a secondary compression stress circle (as shown in Figure 9 (c)), thus forming a deep cable bearing structure (as shown in Figure 9 (d)). The shallow and deep bearing

structures are coupled to form a large range of high stability bolt (cable)-surrounding rock with high strength anchorage bearing structure [29–31]. The surrounding rock in this structure is in three-dimensional compression state, and the residual strength and peak strength of surrounding rock are greatly improved, which can effectively inhibit the development of surrounding rock deformation, control the early attenuation of surrounding rock strength, and ensure the integrity of rock mass in the anchorage area.

The bearing capacity P of the surrounding rock in the anchorage bearing structure area is an important criterion for judging the effect of bolt (cable) support. The calculation formula of bearing capacity P is as follows [32]:

$$P = \frac{2Q_1(1 + \sin \varphi)(l_1 \tan \partial - d_1)}{(d_1)^2 \tan \partial (1 - \sin \varphi)(2R + l_1 - d_1)} + \frac{2Q_2(1 + \sin \varphi)(l_2 \tan \partial' - d_2)}{(d_2)^2 \tan \partial' (1 - \sin \varphi)(2R + l_2 - d_2)}, \quad (1)$$

where Q_1 and Q_2 are prestress of bolt and cable, respectively; φ is the friction angle of anchorage rock mass, 30° ; l_1 and l_2 are the effective length of bolt and cable; d_1 and d_2 are the row spacing of bolt and cable; ∂ , ∂' is the control angle of bolt and cable, 45° ; R is the effective radius of roadway. It can be seen from the formula that the greater the bolt (cable) length, the smaller the row spacing, and the greater the prestress applied, the stronger the bearing capacity of surrounding rock. Only by realizing the optimal combination of bolt (cable) parameters, can the strength of surrounding rock of

the large section chamber group connected with deep shaft be maximized. According to the above analysis and considering the key support parts of each area as shown in Figure 7, the high-strength bolt is applied to the roof, two shoulder angles and two sides of chamber of the each area, and the long cable reinforcement support is applied to the two shoulders and roof of the chamber in areas I, II, III, and IV. Based on this, the support parameters of bolt and cable are determined as follows: (1) the length of bolt is 2400 mm, the diameter is 22 mm, the row spacing is 800×800 mm, the

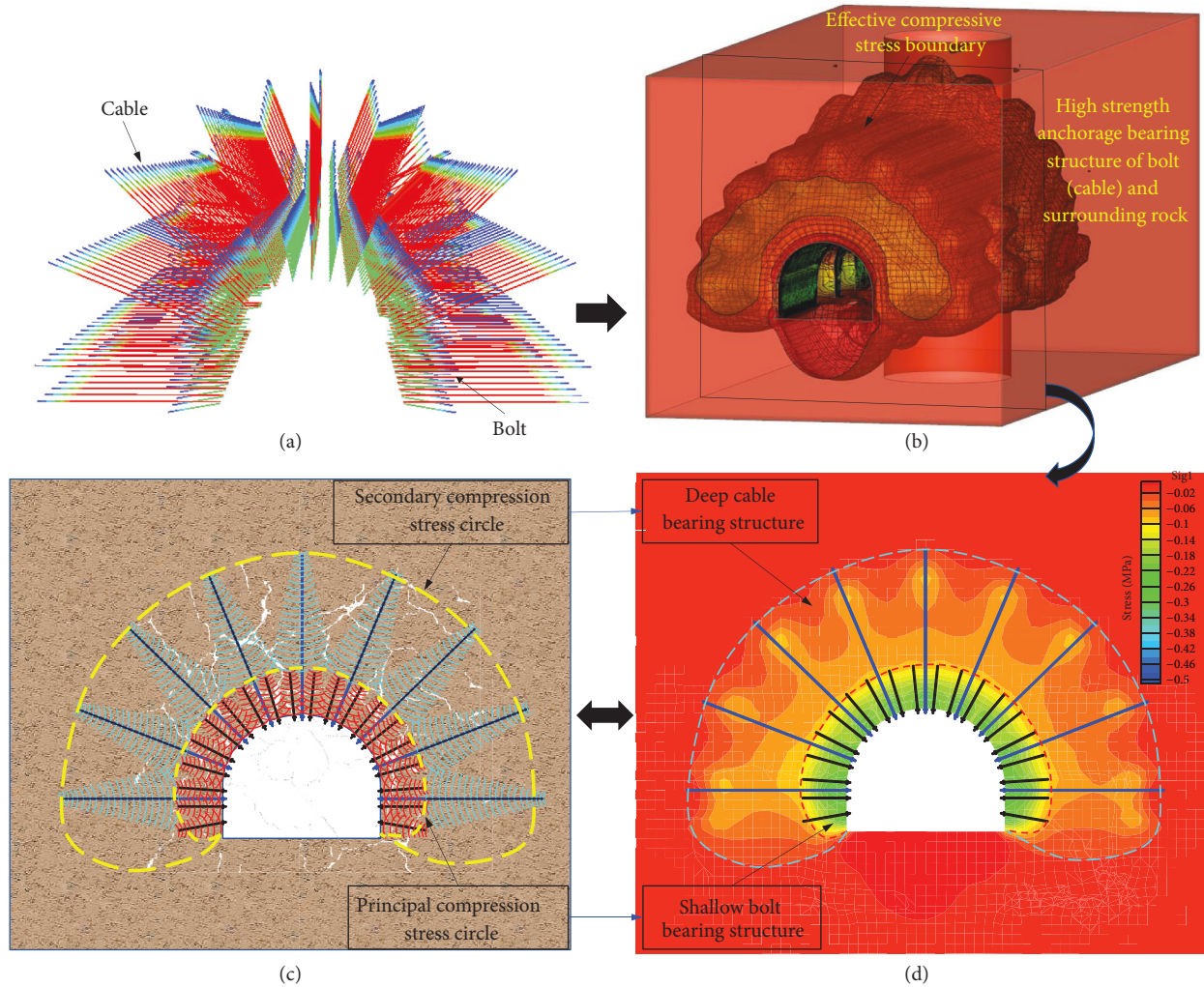


FIGURE 9: High strength anchorage bearing structure: (a) spatial arrangement of bolt (cable), (b) high strength anchorage bearing spatial structure, (c) principal and secondary compression stress circles, and (d) distribution of prestress field of bolt (cable).

pretightening torque is not less than 400 N·m, and the anchoring force is not less than 200 kN. (2) The length of the cable is 8300 mm, the row spacing is 1600 × 800 mm, and the prestress is 200 kN, with minimum anchoring force not less than 250 kN. By substituting the above support parameters into (1), the bearing capacity P under the new support parameters can reach 0.64 MPa. The stability of surrounding rock support system of roadway is significantly improved.

In addition, the shotcreting sealing on the surface of surrounding rock not only improves the stress state of surrounding rock near the surface of roadway, but also protects and reinforces the anchorage bearing structure, which is conducive to the stress diffusion on the surface of surrounding rock, improves the bending stiffness and strength of bearing structure, greatly enhances the ability to resist failure, and effectively limits the development of plastic zone of surrounding rock.

4.2.2. Reinforced Concrete Wall Subarea Brickwork Support Technology. The deformation of surrounding rock of large cross section chamber group connected by deep shaft has the

characteristics of long duration; area uncoordinated deformation; and the deformation of roof, shoulders, and sides in the area is larger than that of floor. Therefore, it is necessary to use reinforced concrete wall brickwork support technology for support roof, shoulders, and sides in each area on the basis of strong bolt (cable) shotcreting support system. Figure 10 shows the numerical calculation models of “bolt-cable-shotcreting support” and “bolt-cable-shotcreting support + reinforced concrete wall brickwork.” Shotcreting is simulated by shell structural element, and reinforced concrete wall brickwork is simulated by solid element. The parameters of support structure are shown in Tables 1–3.

Figure 11 shows the stress distribution curve and plastic distribution diagram of surrounding rock under no support, bolt-cable-shotcreting support (scheme 1), bolt-cable-shotcreting support + reinforced concrete wall brickwork (scheme 2).

It can be seen that the pressure relief range of chamber group under bolt-cable-shotcreting support is smaller than that without support, but the plastic zone of surrounding rock of chamber group is still large under support scheme 1. Only part

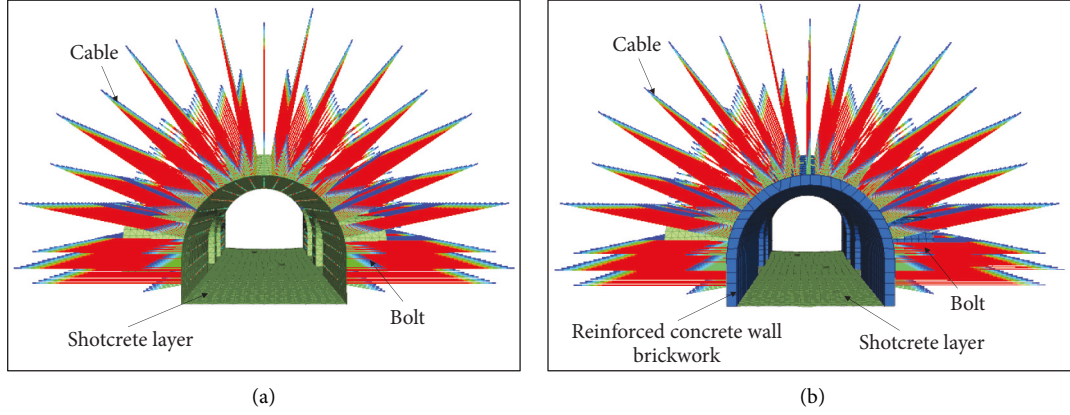


FIGURE 10: Numerical calculation model of support scheme: (a) bolt-cable-shotcreting support and (b) bolt-cable-shotcreting support + reinforced concrete wall brickwork.

TABLE 1: Numerical calculation parameters of reinforced concrete wall brickwork.

Density/kg·cm ⁻³	Elasticity modulus/GPa	Cohesion/MPa	Internal friction angle/°	Poisson's ratio
2650	29	15	52	0.17

of bolts is anchored in stable surrounding rock, the stress of rock column is weak, and the stress concentration degree of surrounding rock of chamber group varies greatly under bolt-cable-shotcreting support. After the reinforced concrete wall brickwork is used for support, through the full contact between the wall brickwork and the surrounding rock, it can provide high lateral pressure to the surrounding rock, realize the real three-dimensional stress state of the shallow surrounding rock, improve the residual strength of the surrounding rock, and control the deformation of the surrounding rock. Scheme 2 (bolt-cable-shotcreting support + reinforced concrete wall brickwork) further realizes the transfer and diffusion of the high concentrated stress in the surrounding rock to the low stress area and enhances the stress of the rock column. The plastic zone of surrounding rock of each chamber is greatly reduced, which can ensure that the bolt is anchored in the stable rock stratum and the anchoring point is firm.

Figure 12 shows the distribution of deviatoric stress of reinforced concrete wall brickwork.

It can be seen from the nephogram that the reinforced concrete wall brickwork is in compression state as a whole. Due to the uncoordinated deformation and failure of each area, the areas III and IV of chamber group are in the low value area of deviatoric stress, and areas I and II are in the peak area and the median area of deviatoric stress, respectively. The deviatoric stress of roof and two shoulder in each area is greater than that of other parts. The deviatoric stress of the roof and shoulders in

the variable section part of area I is the largest, which is 10.2 MPa and 11.3 MPa, respectively. On the whole, the stress difference of reinforced concrete wall brickwork is small and keeps low, and the reinforced concrete wall brickwork is in a stable working state.

4.2.3. Hollow Bolt (Cable) Grouting Reinforcement Technology of Fragmented Coal and Rock Mass. The surrounding rock of large cross section chamber group connected by deep shaft has poor stability and developed bedding. Under the action of deviatoric stress, the surrounding rock is fractured unevenly, and the deformation and failure has regional characteristics. Therefore, according to the specific broken degree of each area, the method of hollow grouting subarea reinforcement can be used to fill and cement the surrounding rock with different fracture states in each area. Grouting can consolidate the broken rock, change the mechanical properties of coal and rock mass, improve the integrity of coal and rock mass, reduce the deformation index of surrounding rock, and realize the further coupling of support and surrounding rock [33–35]. The failure mechanics of rock mass before and after grouting is shown in Figure 13.

According to the literature [36], the maximum shear stress of grouting anchorage rock mass interface is as follows:

$$\tau' = c' + \frac{1}{2}k'(u_m - u_e)\tan \psi' \tan \varphi' + \frac{2(1-u')\lambda^2 q \tan \varphi'}{\lambda^2 + (1-2u') + E'(1-2u)(1+u)(\lambda^2 - 1)/E_m(1+u')}, \quad (2)$$

$$k' = \frac{1}{[(1+u')a/E' + (1+u)(1-2u)a/E]}, \quad c' = c + \Delta c, \psi' = \psi + \Delta \psi, \varphi' = \varphi + \Delta \varphi, E' = E + \Delta E.$$

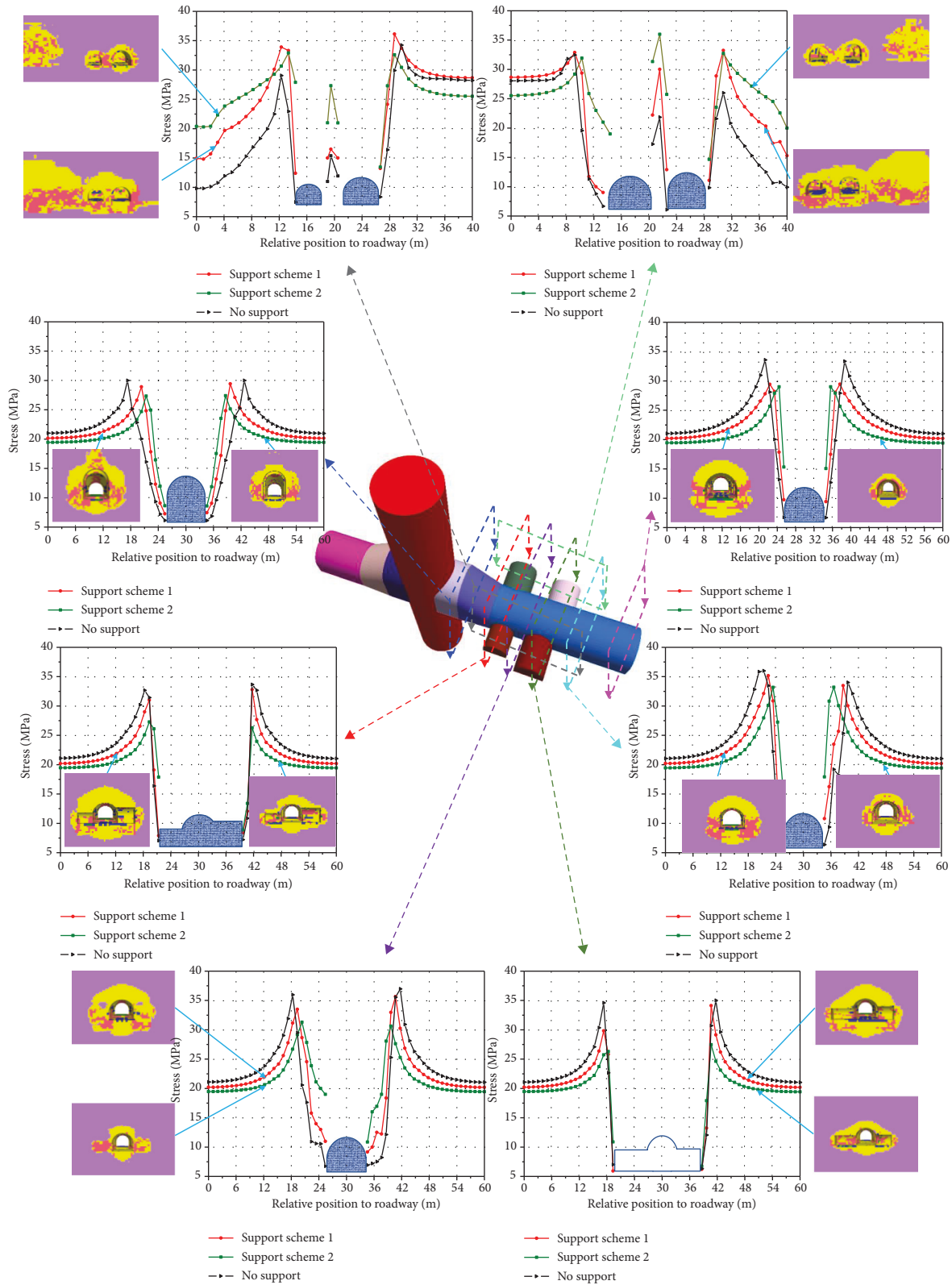


FIGURE 11: Stress distribution curve and plastic distribution diagram of surrounding rock under different support schemes.

According to the formula, with the increase of elastic modulus, cohesion, internal friction angle, and dilatancy angle of surrounding rock, the maximum shear stress of grouting anchorage rock mass interface increases

continuously. It shows that in the weak and broken surrounding rock, the mechanical parameters of rock mass can be improved by means of grouting reinforcement measures, and the shear capacity of anchorage body interface will be

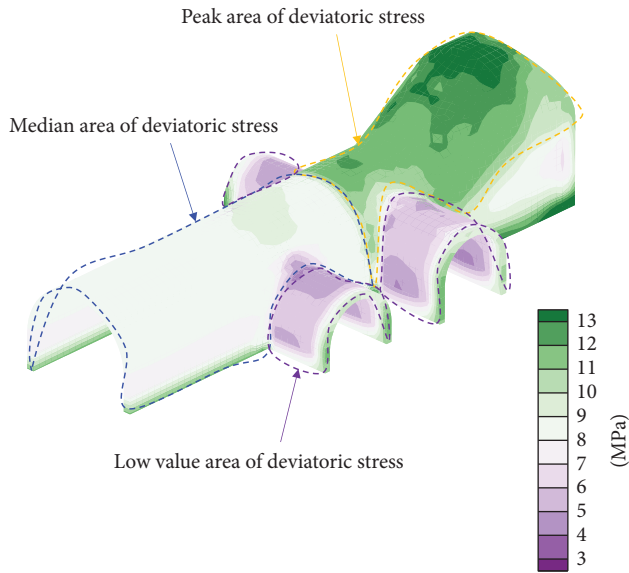


FIGURE 12: Distribution diagram of deviatoric stress of reinforced concrete wall brickwork.

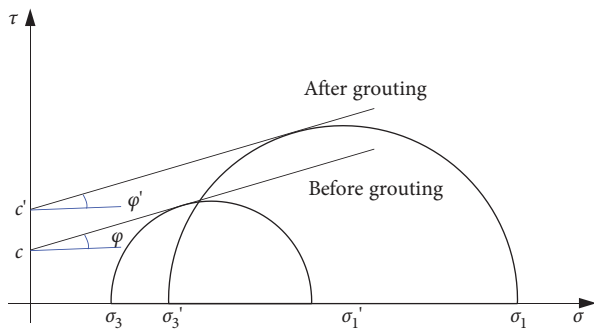


FIGURE 13: Failure mechanics condition of rock mass before and after cable grouting.

improved. Based on the above analysis and according to the key support parts of each area shown in Figure 7, the grouting bolt is applied to rock column wall between chamber in area III and area IV, and hollow grouting long cable is applied to the two shoulders and roof of roadway in areas II, III and IV, and the sides, two shoulders and roof of roadway in area I. In addition, in order to prevent large area floor heave, hollow grouting cable is used to reinforce the floor of area I and II.

5. Engineering Practice

5.1. Determination of Support Scheme Parameters. According to the surrounding rock failure characteristics and control countermeasures and technologies in Sections 2 and 3, the basic control ideas and technical methods of surrounding rock are formed as shown in Figure 14, and the subarea collaborative control technology of “high-strength prestressed bolt (cable) mesh shotcreting coupling + reinforced concrete wall brickwork support technology + high-strength bolt (cable) grouting of fragmented coal and rock mass” is determined.

The bolt is MSGW-500/22 × 2400 mm high strength resin bolt with row spacing of 800 × 800 mm, the tightening torque is not less than 400 N·m, and the anchoring force is not less than 200 kN. The material of cable is SKP22-1 × 19/1860, the length is 8300 mm, the row spacing is 1600 × 800 mm, and the prestress is 200 kN, with minimum anchoring force not less than 250 kN.

The shotcreting thickness of roof and side in each area is 100 mm. The floor shotcreting thickness of area I and II are 300 mm, and the concrete strength grade is C20. The thickness of reinforced concrete wall brickwork in area I, area II, and area III is 600, 500, and 400 mm, respectively. The thickness of reinforced concrete wall brickwork of 1# hydraulic station chamber in area IV is 400 mm. The reinforced concrete wall brickwork is not adopted in waiting chamber. The strength grade of reinforced concrete wall brickwork is C45. The material of grouting cable is SKZ29-1/1770-9300, and the spacing rows is 1600 × 800 mm. The grouting slurry is cement slurry, the water cement ratio is 1 : 2.5, and ACZ-1 grouting additive with 8% cement weight is added into the cement slurry.

The rock pillar is a reinforcement support with counter-pulled cable. After the grouting of the rock column between area III and area IV is completed, a 3700 mm long, 21.8 mm diameter counter-pulled cable is added to the rock column between 2# hydraulic station chamber and waiting chamber, and a 5000 mm long, 21.8 mm diameter counter-pulled cable is added to the rock column between 1# hydraulic station chamber and control chamber. The row spacing is 800 mm × 800 mm. The cable is locked in the side of the chamber, and the tray size is long × wide × thickness = 400 mm × 400 mm × 25 mm. The spatial stereogram of chamber group support scheme is shown in Figure 15.

5.2. Strata Behaviors Observation. In order to test the rationality of support design, monitoring sections are set in the surrounding rock of the chamber group to detect the deformation and cable working resistance after the completion of support in each area.

Taking the typical super large section of maximum deformation area I as an example, the layout of measuring points is shown in Figure 16(a). The deformation of roadway roof, left shoulder, right shoulder, left side, right side, and floor are monitored by measuring points A, B, C, D, E, and F, respectively. The working resistance monitoring results of roof and two shoulder cables of typical super large section in area I are shown in Figure 16(b).

It can be seen from Figure 16(a) that in the first 18 days after the completion of the support, the surrounding rock is in the period of severe deformation, forming the initial large deformation. After 18 days, the support structure and surrounding rock gradually reach the coupling state, the surrounding rock enters the stage of small deformation, the deformation rate of surrounding rock tends to ease, and the surrounding rock returns to stability after 36 days. The maximum deformation of roadway roof, left shoulder angle,

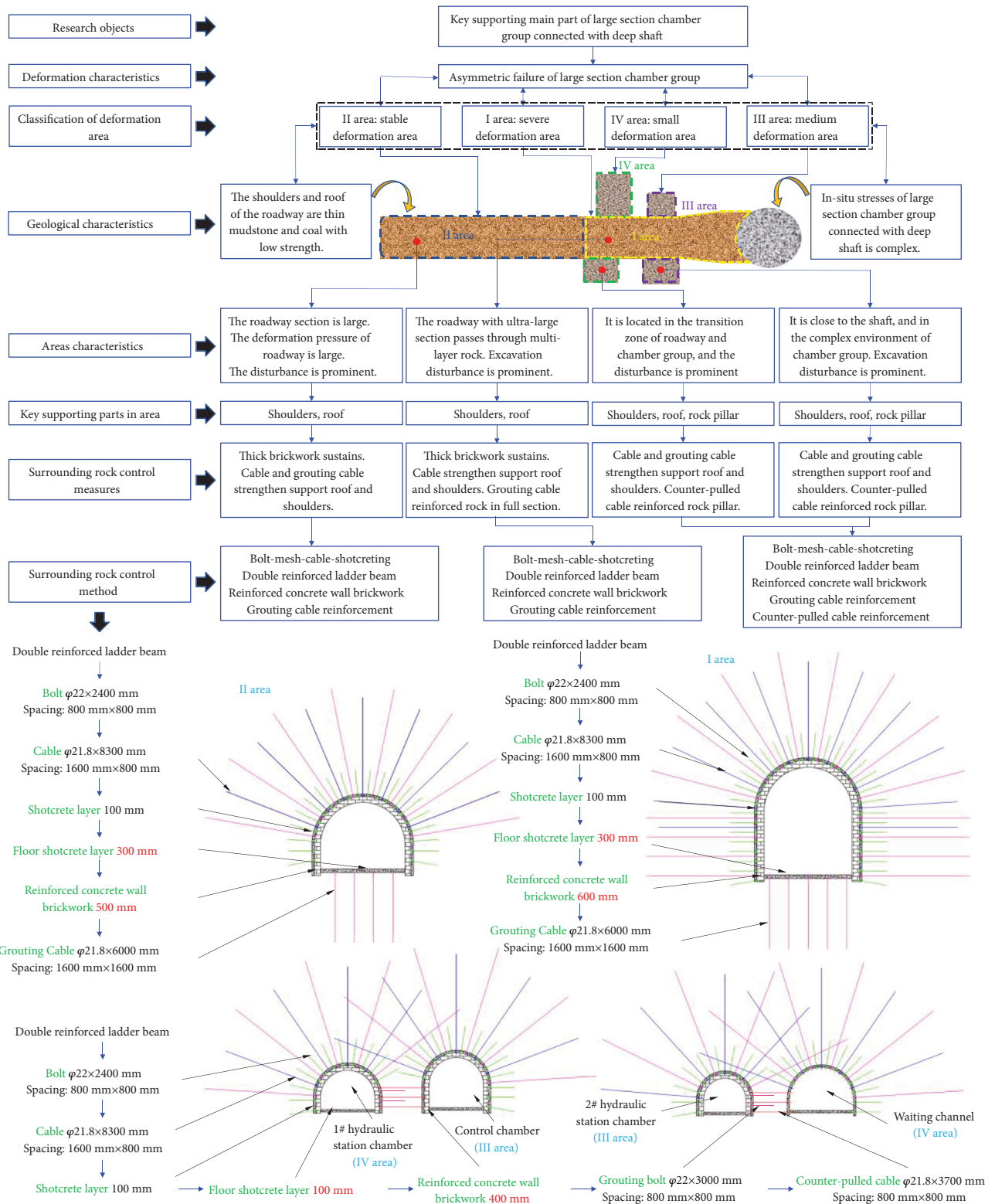


FIGURE 14: Basic control ideas and technical methods of surrounding rock.

right shoulder angle, left side, right side, and floor are 40, 48, 42, 34, 32, and 30 mm. There are some differences in surrounding rock deformation in different areas, but the difference of deformation is controlled within 20 mm. From

Figure 16(b), it can be concluded that the working resistance of cable changes with time is as follows: the stress conditions of cable in different roadway parts are different. After 36 days, the working resistance of cable is relatively stable. The

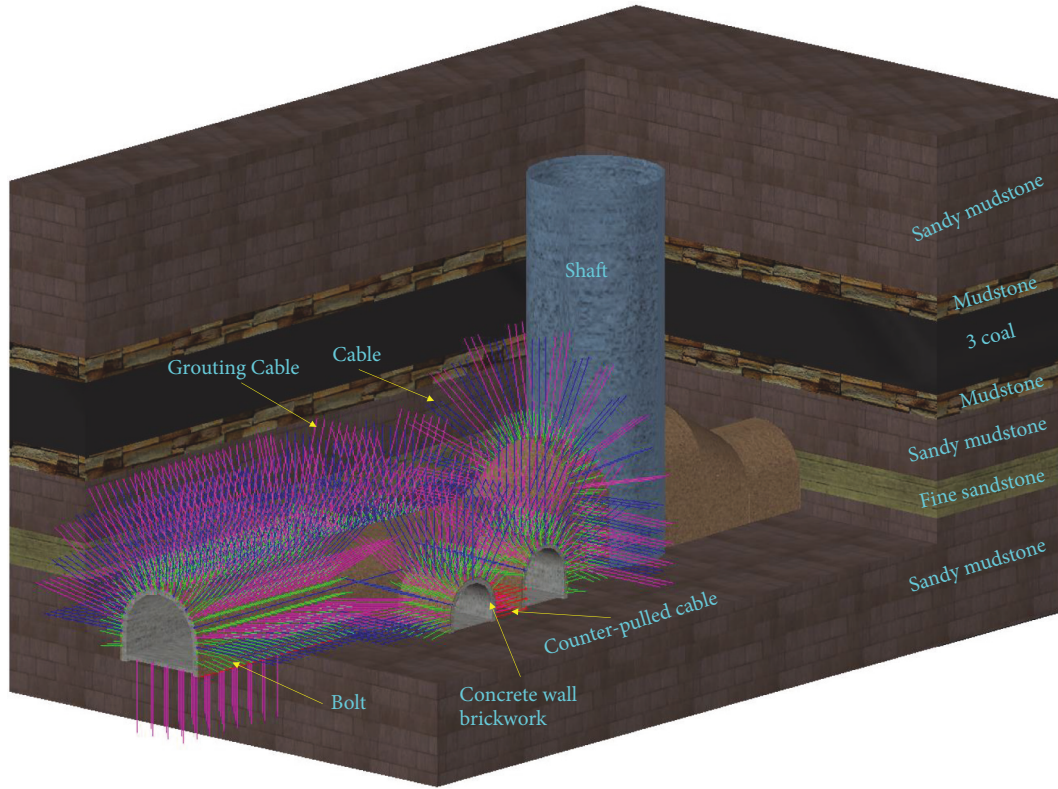


FIGURE 15: Spatial stereogram of support scheme.

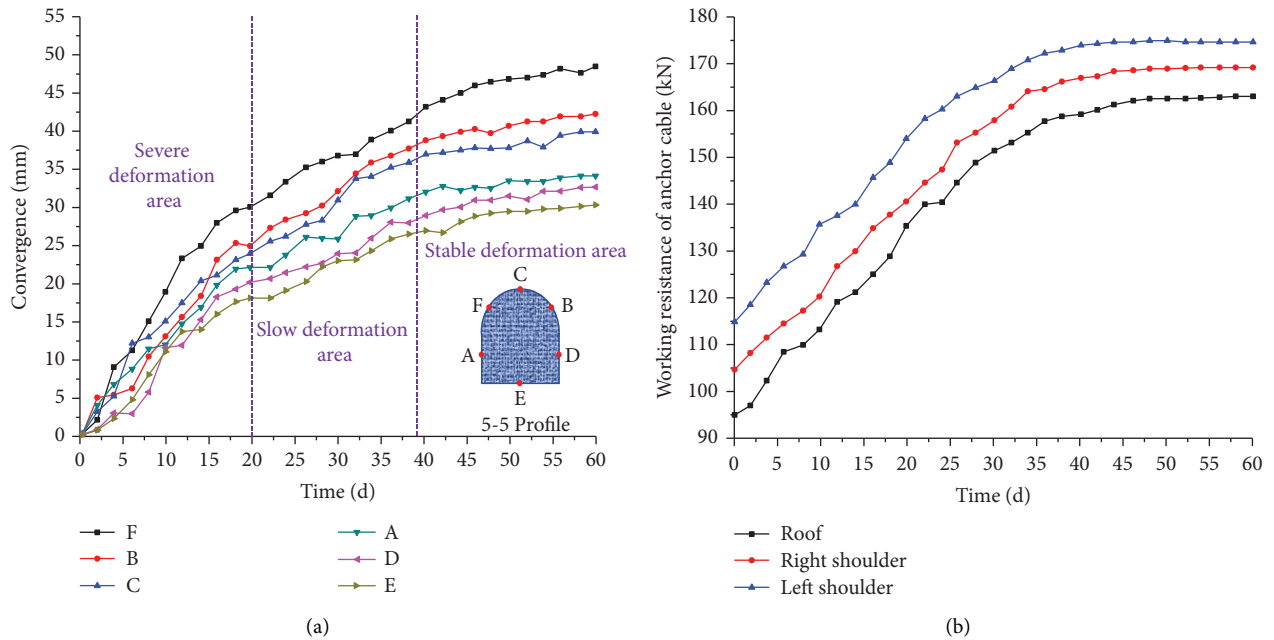


FIGURE 16: Monitoring results of mine pressure in area I. (a) Monitoring results of typical super large section surrounding rock convergence. (b) Cables working resistance monitoring results of typical super large section roof and two shoulder.

TABLE 2: Numerical calculation parameters of bolt/cable.

Supporting structure	Elasticity modulus/ GPa	Cross section area/ 10^{-4} m^2	Adhesion/ $10^5 \text{ N}\cdot\text{m}^{-1}$	Bond stiffness/ $10^7 \text{ N}\cdot\text{m}^{-2}$	Breaking load/ kN
Bolt	210	9.43	4.2	2.51	231
Cable	196	9.43	1.8	1.19	580

TABLE 3: Numerical calculation parameters of shotcreting.

Elasticity modulus/GPa	Poisson's ratio	Cohesion/MPa	Internal friction angle/°	Thickness/mm	Normal stiffness/ $10^8 \text{ N}\cdot\text{m}^{-3}$	Tangential stiffness/ $10^8 \text{ N}\cdot\text{m}^{-3}$
26	0.21	3.2	51	100 (floor) 300 (side and roof)	8	8

maximum working resistance of cable in roof, left shoulder, and right shoulder are 163, 175, and 169 kN, respectively, and the working resistance of cable is in the normal range, realizing effective control of surrounding rock of large section chamber group.

6. Conclusion

- (1) There are obvious differences in the failure of surrounding rock of super large section soft rock chamber group connected by deep vertical shaft. Generally, the degree of deformation and failure from large to small is as follows: the variable section super large section roadway from the waiting chamber (1# hydraulic chamber) to the shaft (area I: severe deformation area), the roadway close to the waiting chamber (1# hydraulic chamber) and gradually away from the shaft (area II: stable deformation area), the 2# hydraulic chamber and control chamber (area III: medium deformation area), and 1# hydraulic chamber and waiting chamber (area IV: small deformation area). The broken degree of roof and two shoulders of surrounding rock is greater than that of the two sides. So the roof and two shoulders of surrounding rock is the key supporting part.
- (2) When considering the support design of surrounding rock of super large section soft rock chamber group connected by deep vertical shaft, the support strength should be reasonably formulated according to the different damage degree of surrounding rock in each area of chamber group. The support concept of zoning cooperative control of large section soft rock chamber group is put forward. The subarea collaborative control technology of "high-strength prestressed bolt (cable) mesh shotcreting coupling + reinforced concrete wall brickwork support technology + high-strength bolt (cable) grouting of fragmented coal and rock mass" is determined.
- (3) After the completion of the new support, the deformation rate of surrounding rock tends to ease, and the surrounding rock returns to stability after 36 days. The maximum deformation of roadway roof, left shoulder angle, right shoulder angle, left side, right side and floor are 40, 48, 42, 34, 32, and 30 mm. After 36 days, the working resistance of cable is relatively stable. The maximum working resistance of cable in roof, left shoulder, and right shoulder are 163, 175, and 169 kN, respectively, and the working resistance of cable is in the normal range, realizing effective control of surrounding rock of large section chamber group.

7. Discussion

Aiming at solving the problem of asymmetric deformation, failure, and stability control of surrounding rock caused by the excavation of deep super large section soft rock chamber group passing through multilayer strata, the deformation development mode of surrounding rock, the expansion situation of loosening range, and the plastic failure response characteristics in chamber group under the disturbance influence are monitored and numerically analyzed in this paper. On this basis, the super large section chamber group is divided into four maintenance control areas: area I (severe deformation area), area II (stable deformation area), area III (medium deformation area), and area IV (small deformation area), and the asymmetric deformation and failure mechanism of the surrounding rock of the chamber group is analyzed. The basic control ideas and technical methods of surrounding rock of deep large section soft rock chamber group are formed. The subarea collaborative control technology of "high-strength prestressed bolt (cable) mesh shotcreting coupling + reinforced concrete wall brickwork support technology + high-strength bolt (cable) grouting of fragmented coal and rock mass" is proposed. The research results obtained in this paper can be applied to the control of surrounding rock of super large section soft rock chamber group connected by deep vertical shaft and can provide reference for the support design of roadway surrounding rock control under similar geological conditions. However, this study has the following shortcomings: this study mainly carries out the research work through engineering practice, field measurement, numerical simulation, and theoretical analysis. So, this paper lacks certain laboratory experiment. In the future research work, more comprehensive research methods should be used to carry out the research work.

Data Availability

The data in this paper were obtained by field measurement and laboratory test.

Conflicts of Interest

The authors declare no conflicts of interest.

Acknowledgments

This work was supported by the National Natural Science Foundation of China (nos. 52074296 and 52004286), the China Postdoctoral Science Foundation (no. 2020T130701), and the Fundamental Research Funds for the Central Universities (nos. 2022XJNY02 and 2022YJSNY18).

References

- [1] R. Knapstein, G. Kuenne, L. G. Becker et al., "Large eddy simulation of a novel gas-assisted coal combustion chamber," *Flow, Turbulence and Combustion*, vol. 101, no. 3, pp. 895–926, 2018.
- [2] M. Li, S. M. Aminossadati, and C. Wu, "Numerical simulation of air ventilation in super-large underground developments," *Tunnelling and Underground Space Technology*, vol. 52, pp. 38–43, 2016.
- [3] G. Zhang, S. Liang, Y. Tan, F. Xie, S. Chen, and H. Jia, "Numerical modeling for longwall pillar design: a case study from a typical longwall panel in China," *Journal of Geophysics and Engineering*, vol. 15, no. 1, pp. 121–134, 2018.
- [4] W. Zhu, J. Xu, and Y. Li, "Mechanism of the dynamic pressure caused by the instability of upper chamber coal pillars in Shendong coalfield, China," *Geosciences Journal*, vol. 21, no. 5, pp. 729–741, 2017.
- [5] W. Yu and K. Li, "Deformation mechanism and control technology of surrounding rock in the deep-buried large-span chamber," *Geofluids*, vol. 2020, pp. 1–22, 2020.
- [6] M. J. Ajrash, J. Zanganeh, and B. Moghtaderi, "Methane-coal dust hybrid fuel explosion properties in a large scale cylindrical explosion chamber," *Journal of Loss Prevention in the Process Industries*, vol. 40, pp. 317–328, 2016.
- [7] X. Sun, B. Zhang, Z. Tao, C. Zhao, and J. Wang, "Research on supporting measure at intersection of inclined shaft and major tunnel in highway," *Advances in Civil Engineering*, vol. 2020, pp. 1–15, 2020.
- [8] B. Zhang, D. Zhai, and W. Wang, "Failure mode analysis and dynamic response of a coal mine refuge chamber with a gas explosion," *Applied Sciences*, vol. 6, no. 5, p. 145, 2016.
- [9] X. Zhai, G. Huang, C. Chen, and R. Li, "Combined supporting technology with bolt-grouting and floor pressure-relief for deep chamber: an underground coal mine case study," *Energies*, vol. 11, no. 1, p. 67, 2018.
- [10] E. Wang and S. Xie, "Determination of coal pillar width for gob-side entry driving in isolated coal face and its control in deep soft-broken coal seam: a case study," *Energy Science & Engineering*, vol. 2022, pp. 1–12, 2022.
- [11] W. Zhai, Y. Guo, X. Ma et al., "Research on hydraulic fracturing pressure relief technology in the deep high-stress roadway for surrounding rock control," *Advances in Civil Engineering*, vol. 2021, pp. 1–13, 2021.
- [12] R. S. Yang, H. J. Xue, D. M. Guo, Y. L. Li, T. T. Li, and J. Z. Xue, "Failure mechanism of surrounding rock of large section chambers in complex rock formations and its control," *Journal of China Coal Society*, vol. 40, no. 10, pp. 2234–3224, 2015, in Chinese.
- [13] S. Xie, E. Wang, D. Chen et al., "Failure analysis and control mechanism of gob-side entry retention with a 1.7-m flexible-formwork concrete wall: a case study," *Engineering Failure Analysis*, vol. 117, Article ID 104816, 2020.
- [14] S. R. Xie, E. Wang, D. D. Chen, Z. S. Jiang, H. Li, and R. P. Liu, "Collaborative control technology of external anchor-internal unloading of surrounding rock in deep large-section coal roadway under strong mining influence," *Journal of China Coal Society*, vol. 47, no. 5, pp. 1946–1957, 2022, in Chinese.
- [15] Y. J. Zhang, X. T. Feng, and Q. Jiang, "Uncertainty analysis and risk management of underground chamber group at Jinping II hydropower station," *Geotechnical Safety and Risk V*, pp. 645–651, 2016.
- [16] X. Ding, X. Niu, Q. Pei, S. Huang, Y. Zhang, and C. Zhang, "Stability of large underground caverns excavated in layered rock masses with steep dip angles: a case study," *Bulletin of Engineering Geology and the Environment*, vol. 78, no. 7, pp. 5101–5133, 2019.
- [17] H.-X. Wang, B. Zhang, D. Fu, and A. Ndeunjema, "Stability and airtightness of a deep anhydrite cavern group used as an underground storage space: a case study," *Computers and Geotechnics*, vol. 96, pp. 12–24, 2018.
- [18] B. Zhang, H. Wang, L. Wang, and N. Xu, "Stability analysis of a group of underground anhydrite caverns used for crude oil storage considering rock tensile properties," *Bulletin of Engineering Geology and the Environment*, vol. 78, no. 8, pp. 6249–6265, 2019.
- [19] Y. B. Huang, Q. Wang, H. K. Gao, Z. H. Jiang, K. Li, and K. Chen, "Failure mechanism and construction process optimization of deep soft rock chamber group," *Journal of China University of Mining & Technology*, vol. 50, no. 01, pp. 69–78, 2021, in Chinese.
- [20] Q. Wang, H. J. Zhang, B. Jiang et al., "Failure mechanism of deep large section chamber and anchor injection control method," *Journal of Mining & Safety Engineering*, vol. 37, no. 06, pp. 1094–1103, 2020, in Chinese.
- [21] L. Xu, T. Zhang, and Q. Ren, "Intelligent autofeedback and safety early-warning for underground cavern engineering during construction based on bp neural network and fem," *Mathematical Problems in Engineering*, vol. 2015, pp. 1–8, 2015.
- [22] Q. Qian and X. Zhou, "Failure behaviors and rock deformation during excavation of underground cavern group for jinping I hydropower station," *Rock Mechanics and Rock Engineering*, vol. 51, no. 8, pp. 2639–2651, 2018.
- [23] X. Liu, S. Song, Y. Tan et al., "Similar simulation study on the deformation and failure of surrounding rock of a large section chamber group under dynamic loading," *International Journal of Mining Science and Technology*, vol. 31, no. 3, pp. 495–505, 2021.
- [24] L. Zhou, Y. Huang, Z. Shao, F. Ma, P. Zhang, and Y. Wang, "Research on surrounding rock rheological effect and control method of large section chamber group in deep well," *Geotechnical & Geological Engineering*, vol. 39, no. 7, pp. 5041–5061, 2021.
- [25] Y. Tan, D. Fan, X. Liu, S. Song, X. Li, and H. Wang, "Numerical investigation of failure evolution for the surrounding rock of a super-large section chamber group in a deep coal mine," *Energy Science & Engineering*, vol. 7, no. 6, pp. 3124–3146, 2019.
- [26] F. Zhang, J. Liu, X. Zhang, H. Ni, and Y. Liu, "Research on excavation and stability of deep high stress chamber group: a case study of Anju Coal Mine," *Geotechnical & Geological Engineering*, vol. 39, no. 5, pp. 3611–3626, 2021.
- [27] W. Yu, K. Li, Z. Liu, B. An, P. Wang, and H. Wu, "Mechanical characteristics and deformation control of surrounding rock in weakly cemented siltstone," *Environmental Earth Sciences*, vol. 80, no. 9, p. 337, 2021.
- [28] W. Yu, G. Wu, B. Pan, Q. Wu, and Z. Liao, "Experimental investigation of the mechanical properties of sandstone-coal-bolt specimens with different angles under conventional triaxial compression," *International Journal of Geomechanics*, vol. 21, no. 6, Article ID 04021067, 2021.
- [29] J. Chen, H. Zhao, F. He, J. Zhang, and K. Tao, "Studying the performance of fully encapsulated rock bolts with modified structural elements," *International Journal of Coal Science & Technology*, vol. 8, no. 1, pp. 64–76, 2021.
- [30] A. Batugin, Z. Wang, Z. Su, and S. S. Sidikova, "Combined support mechanism of rock bolts and anchor cables for

- adjacent roadways in the external staggered split-level panel layout,” *International Journal of Coal Science & Technology*, vol. 8, no. 4, pp. 659–673, 2021.
- [31] J. Chang, K. He, D. Pang, D. Li, C. Li, and B. Sun, “Influence of anchorage length and pretension on the working resistance of rock bolt based on its tensile characteristics,” *International Journal of Coal Science & Technology*, vol. 8, no. 6, pp. 1384–1399, 2021.
- [32] W. J. Yu, Q. Gao, and C. Q. Zhu, “Study of strength theory and application of overlap arch beating body for deep soft surrounding rock,” *Chinese Journal of Rock Mechanics and Engineering*, vol. 29, no. 10, pp. 2134–2142, 2010, in Chinese.
- [33] H. Yu, H. Jia, S. Liu, Z. Liu, and B. Li, “Macro and micro grouting process and the influence mechanism of cracks in soft coal seam,” *International Journal of Coal Science & Technology*, vol. 8, no. 5, pp. 969–982, 2021.
- [34] S. Li, C. Ma, R. Liu et al., “Super-absorbent swellable polymer as grouting material for treatment of karst water inrush,” *International Journal of Mining Science and Technology*, vol. 31, no. 5, pp. 753–763, 2021.
- [35] S. Xie, Y. Wu, D. Chen, R. Liu, X. Han, and Q. Ye, “Failure analysis and control technology of intersections of large-scale variable cross-section roadways in deep soft rock,” *International Journal of Coal Science & Technology*, vol. 9, no. 1, p. 19, 2022.
- [36] Q. Wang, Q. Qin, B. Jiang, H. C. Yu, R. Pan, and S. C. Li, “Study and engineering application on the bolt-grouting reinforcement effect in underground engineering with fractured surrounding rock,” *Tunnelling and Underground Space Technology*, vol. 84, pp. 237–247, 2019.